Q. J. R. Meteorol. Soc. (1997), **123**, pp. 1707-1724

The tropical stratopause in the UKMO stratospheric analyses: Evidence for a 2-day wave and inertial circulations.

By YVAN J. ORSOLINI[1*], VARAVUT LIMPASUVAN[2], and CONWAY B. LEOVY[2]
[1] *Centre National de Recherches Météorologiques, France*
[2] *University of Washington, USA*

(Received 12 April 1996; revised 9 December 1996)

Summary

Large-scale atmospheric motions near the low latitude stratopause in the UK Meteorological Office stratospheric analyses during the northern hemisphere winter are investigated, focusing in particular on the 2-day wave and inertial eddies.

The 2-day wave is a westward propagating planetary wave which appears recurrently in the summer subtropical upper stratosphere and mesosphere. Space-time spectral analysis of the assimilated fields of temperature and winds, and high-resolution transport of water vapour, reveal large-amplitude breaking planetary waves in the summer subtropics, principally a 2-day wave 3 and a wave 1 of a period near 7 days. A region of anomalous zonal-mean meridional gradient of potential vorticity also exists, pointing to a barotropic instability mechanism for the origin of the 2-day wave.

By contrast, the winter subtropics are characterized by mixing on less-than-planetary scales during the period considered, occurring during the easterly phase of the stratospheric semi-annual oscillation. Water vapour is mixed turbulently into gyres, and drawn in narrow filaments out of the southern hemisphere. The potential vorticity field displays vertically layered, zonally-asymmetric variations.

The behaviour of the model assimilated fields is supported by along-track water vapour distribution observed by the Microwave Limb Sounder aboard the Upper Atmosphere Research Satellite shows evidences for intermittent filamentary mixing in the northern subtropics, and a 2-day wave signature in the summer subtropics.

Based on these results, a possible mechanism connecting the initiation of the austral 2-day wave events to strong planetary wave activity in the winter is proposed. The winter planetary waves provide the background conditions for development of inertial instabilities at low latitudes of the winter hemisphere, which in turn create conditions favourable for barotropic instability of the summer subtropical easterly jet.

Keywords: Barotropic instability Inertial instability Middle atmosphere Planetary-wave breaking

1. Introduction

Global meteorological analyses of the middle atmosphere are increasingly used for transport studies of trace constituents. It is important to assess whether they accurately represent the major features of atmospheric circulation. This is specially true in the tropics, where the winds are not easily derived from temperature through a balance relation, where unique dynamical phenomena occur, and where barriers to transport from high latitudes are sometimes found. The UK Meteorological Office (UKMO) stratospheric analyses are made available to the scientific community as a correlative analysis tool for the Upper Atmosphere Research Satellite (UARS) mission. In this paper, we examine whether these analyses include two major features of the circulation in the tropical upper stratosphere, lower mesosphere region: the 2-day waves and inertial circulations.

The 2-day wave is a planetary scale westward propagating wave, characterized by a period of about 48-49 hours. It appears recurrently in the summer subtropics shortly after the summer solstice, i.e. when

* Corresponding author: Météo-France, CNRM/ERAM, 42 avenue G. Coriolis, 31057 Toulouse Cedex, France

the westward jet is the strongest (January-February in the southern hemisphere, SH). It has dominant zonal wave numbers 3 or 4; in the northern hemisphere (NH), its period is slightly longer (51-52 hours), and its magnitude smaller on average. The 2-day wave signature in winds or temperature has been detected in radar, rocketsonde and satellite data (see Plumb (1983), or Randel (1994) for reviews). Recently, Limpasuvan and Leovy (1995, hereafter LL95) have detected its presence in the UARS Microwave Limb Sounder (MLS) temperature measurements gathered in January and February 1992. Furthermore, they have for the first time shown its signature on an atmospheric tracer which has a strong gradient across the subtropical jet, namely on water vapour. A 2-day wave signature was also seen in January 1992 in the mesosphere and lower thermosphere in data from the High Resolution Doppler Imager aboard UARS (Wu *et al.*, 1993).

During the season when the 2-day waves are active in the summer hemisphere, vertically layered zonally asymmetric temperature perturbations have been analyzed in data from the Limb Infrared Monitor of the Stratosphere (LIMS) instrument which operated from November 1978 to May 1979. These features were found near the stratopause, persisted as low wave number stationary disturbances over times of order of a week, and were associated with week-to-week variations in the strength of the equatorial meridional circulations and strong planetary wave driving of the mean flow (Hitchman *et al.*, 1987; Hitchman and Leovy, 1986). The disturbances occur in association with the easterly phase of the semiannual oscillation in the region where zonal mean easterlies extend into the winter hemisphere. Hitchman *et al.* proposed that these features were signatures of inertially unstable waves and pointed out that they should act to effectively mix potential vorticity across the winter tropical region. It should be noted that the LIMS data and analysis methods were only capable of identifying low zonal wave number structures, and that the actual disturbances could contain higher zonal wave number components.

In this paper, we examine dynamical phenomena near the low latitude stratopause, focusing on the austral summer season with particular emphasis on the period from December 1991 through February 1992. First, a spectral analysis is performed to search for evidence of the 2-day wave and to identify its zonal wave number components. Then, we use UKMO winds to carry out off-line isentropic transport calculations of a passive tracer. The Lagrangian transport of tracer vividly illustrates the nature of the large-scale eddies at low latitudes and their interactions. Both the spectral analysis and the transport calculations reveal 2-day waves that actively mix water vapour across low latitudes of the summer hemisphere. In addition, some passive tracer is transported across the equator as a result of the mixing action of anticyclonic gyres of high zonal wave number embedded in the inertially unstable region where easterlies have penetrated into the winter hemisphere. We show that the gyres revealed by the transport calculations are also indicated by dynamically self-consistent fields of winds and potential vorticity (PV). We also examine UARS MLS observations of water vapour near the stratopause during December 1991 to February 1992 and show that the along-track data near the stratopause level shows evidence for intense and thin-scale filamentary mixing in the northern subtropics.

The connections revealed between the mean zonal flow, 2-day waves, inertially unstable gyres, and winter hemisphere planetary wave activity lead us to propose a mechanism linking these through potential vorticity mixing and consequent modification of the mean flow.

In Section 3 we present our discussion and analysis of 2-day wave features, including analyses of data from 3 northern hemisphere winters subsequent to 1991/1992. Evidence for inertially unstable gyres is presented in Section 4. In Section 5, we discuss the UARS MLS water vapour measurements and discuss their relationship to the transport calculation using UKMO winds, and in Section 6, we discuss our proposed mechanism linking these phenomena.

2. THE UKMO STRATOSPHERIC ANALYSES

The UKMO stratospheric analyses are a global dataset covering the troposphere and the middle atmosphere, produced by data assimilation into a general circulation model. They are made available to the scientific community as a correlative analysis tool for the UARS mission. An extensive description can be found in Swinbank and O'Neill (1994a). They have been shown to contain, at low latitudes, clear quasi-biennial and semi-annual oscillations (Swinbank and O'Neill, 1994b).

The only upper-stratospheric measurements assimilated in the version of UKMO analyses used here, are temperature soundings from the National Oceanic and Atmospheric Administration (NOAA) polar-orbiting satellites. Near the stratopause, temperatures in the two vertical layers 0.4-1 mb, and 1- 2 mb, are assimilated. The analyzed winds are gridded every 2.5˚ in latitude, and every 3.75˚ in longitude. It is important to note that the UKMO-UARS analyses are archived on the 22 standard UARS levels, equally spaced in log pressure, and not on the 42 levels of the model in which the temperature observations are assimilated. The UARS levels relevant to this study are at 0.32, 0.46, 0.68, 1.0, 1.46 and 2.1 mb. The general circulation model into which the data are assimilated has 10 levels above 2 mb, but only 5 standard UARS levels are located above that level.

3. THE 2-DAY WAVE IN THE SUMMER SUBTROPICS

(a) Spectral analysis of temperature and winds

Daily temperature and meridional wind fields at 1 mb are spectrally analyzed for a 32-day period starting from 12 January 1992 (UARS day 123). The time series are tapered at each end with a split cosine window, covering 8 days. The spectral resolution is then 1/48, or 0.0208, cycles per day. Power spectra are resolved into eastward and westward components, and then smoothed with a 1/4-1/2-1/4 recursive filter. The shortest resolvable period being 2 days, some power in 2-day wave will be aliased into eastward components (see Randel, 1994).

Figure 1(a) shows the power spectra of the temperature at 20˚S for the four gravest zonal wave numbers, while Figure 1(b) shows the corresponding wind spectra at 10˚S.

The temperature spectra are dominated by westward propagating waves: strong signals correspond to a wave 1 of period near 7 days, and to a wave 3 at a period near 2 days. Two such waves were found in the MLS temperature record for the same period by LL95. They found that the wave 1 maximized in mid-latitudes near 2 mb. In the velocity spectra, the 2-day wave appears clearly as well at wave number 3. In both the temperature and wind spectra, there is some power at wave number 4 in a period range of 2 to 3.5 days.

Figure 1(c) shows the temperature variance time series, resynthesized over the periods ranging from 2.5 to 2 days, and over wave number 3. At 20˚S, the 2-day wave appears as a pulse during January, with a variance peaking at about 1.5 K^2.

(b) Isentropic transport of water vapour during 2-day wave events

Water vapour can be considered as a passive tracer on the time scales of the upper stratospheric and mesospheric circulations described in this paper. Isentropic transport simulations of an idealized tracer, which mimics water vapour, were performed in an off-line manner for two 7-day periods in January 1992 at 1800 K (near 1 mb). The model resolution is about 1˚, and it is described in Orsolini (1995). The tracer is initialized as the zonally-averaged time-averaged water vapour observed by MLS over a ten-day period, starting on 15 January 1992 (UARS days 126-136). Over the course of the integration, the tracer field is distorted by large-scale waves present in the daily isentropic wind fields. A first integration covers 10-17 January (UARS days 121-128, period A), and a second one 20-27 January (UARS days 131-138, period B). Figures 2 (a) and (b) show the tracer field on 15 and 17 January (12 GMT), and Fig. 2(c) on 25 January (12 GMT).

The tracer distribution in Figs. 2(a) and (b) shows clearly a planetary scale disturbance, containing mostly wave numbers 3 and 1, in the southern subtropics. This confirms the results of section 3(a), despite

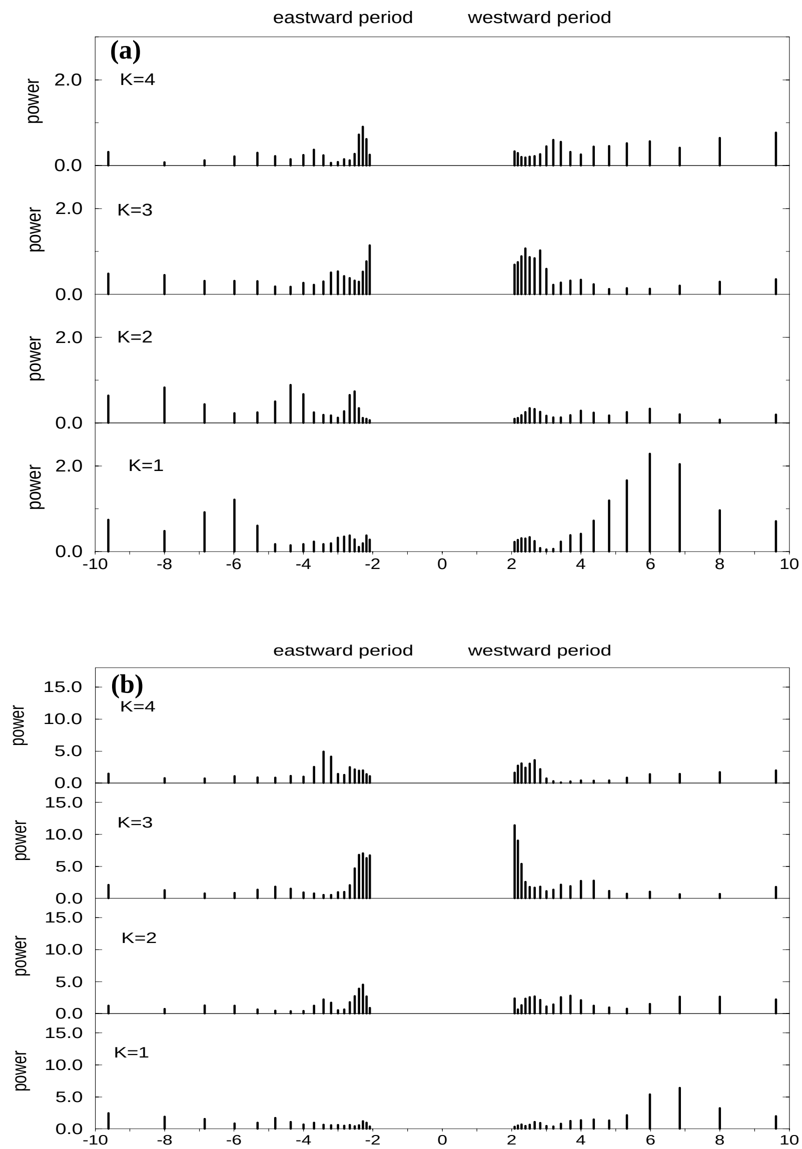

Figure 1. (a) Power spectra of temperature (K) for a 32-day period starting 12 January 1992, at 20˚S and 1 mb, for zonal wave numbers 1 to 4, resolved into eastward and westward components. (b) Same as (a) but for meridional wind at 10˚S. Periods are in days, and the spectral power density is in units of $N \times 10^{-3}$ for K^2 days (or $m^2 s^{-2}$ for velocity), where N is the number of data points. (c) Time series of temperature variance at 1 mb (in K^2) filtered for wave number 3, and periods between 2.5 and 2 days.

uncertainties inherent to spectral analysis of time series near the Nyquist frequency. The waves' westward propagation and period can be inferred from Figs. 2(a) and (b): on 15 January, the western-most wavecrest, e.g. at 10˚S, is near 40˚E; two days later the same crest can be found near 300˚E, while another one is found near 40˚E. The presence of a 2-day wave 3 is particularly strong during period A, while during period B, the wave 1 is the most prominent. The waves in the tracer field are of large amplitudes, and evidence of breaking is seen near the equator. The meridional velocity variance, associated with the 2-day

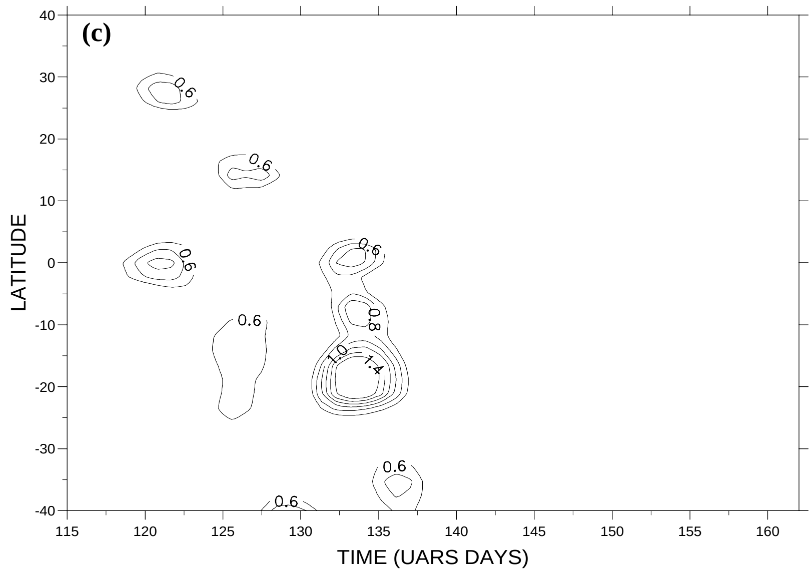

Figure 1. Continued

wave, maximizes at 10˚S on 15 January (UARS day 126).

(c) Potential vorticity and mean-flow structure during 2-day wave events

The upper-left panel on Fig. 3 shows the seasonal evolution of the zonal-mean zonal wind at 1 mb from 10 December 1991 (UARS day 90) through February 1992. Note that a sudden warming event in mid-January was captured by the analyses (Farman *et al.*, 1994). The 2-day wave event (see red dot on Fig. 3 near UARS day 133) peaks shortly after the subtropical jet reaches its maximum amplitude. There is a strong penetration of the easterly regime into the NH, the zero-wind line being pushed to 20˚N. Figure 3 also shows when and where in the southern hemisphere does the zonal mean quasi-geostrophic PV meridional gradient reverse sign (white contours). This is the necessary condition for quasi-geostrophic instability of the zonal mean flow. Such sign reversals occur near 10˚S as the jet builds up in strength.

A latitude/pressure cross-section of the zonally-averaged PV, averaged over a one-week period (UARS days 126-132), on Fig. 4(a), shows that this region of reversed PV gradient is confined near the stratopause.

To further diagnose the unstable character of the flow, we show on Fig. 4(b) that the reversal of the PV gradient is caused by strong meridional wind curvatures, exceeding the beta parameter. Hence, our results point toward a barotropic instability origin.

(d) Results for other UARS years

The analysis is repeated for the 3 following NH winters (UARS days 456-536, 821-901, and 1186-1266). The NH hemisphere zonal-mean jet is much more variable interannually than his SH counterpart. Note the absence of a major sudden warming in 1992/1993.

A 2-day wave in temperature has been found for all the years analyzed, with a peak temperature vari-

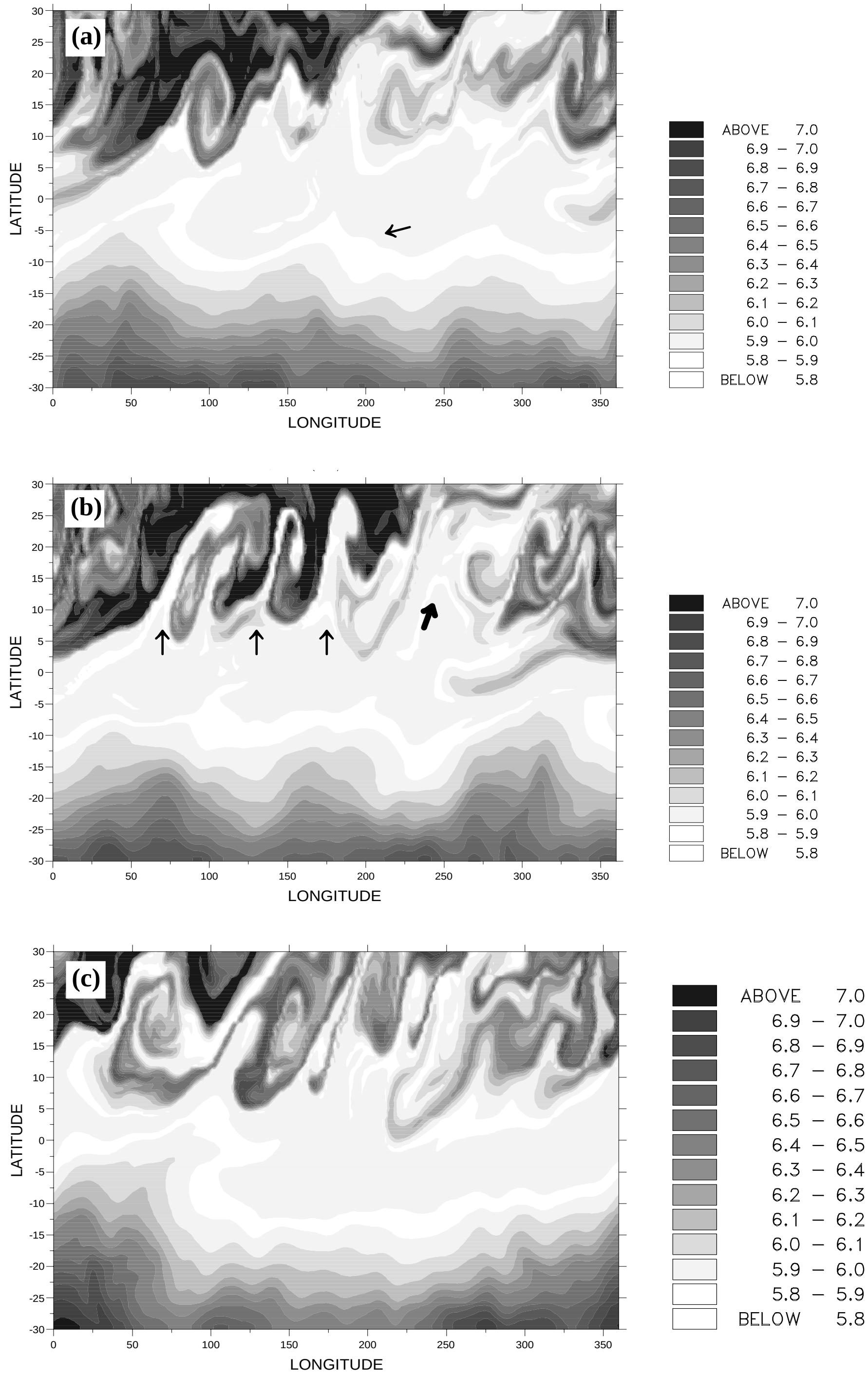

Figure 2. Model tracer distribution of water vapour (p.p.m.v.) at 1800 K at 12 GMT on (a) 15 January, (b) 17 January, and (c) 25 January 1992. On (a) the arrow locates the 2-day wave. On (b) the thick arrow indicates the dry tongue eroded out of the tropics, while the thin arrows point toward high wave number eddied (see text). Note the uneven spacing of contours.

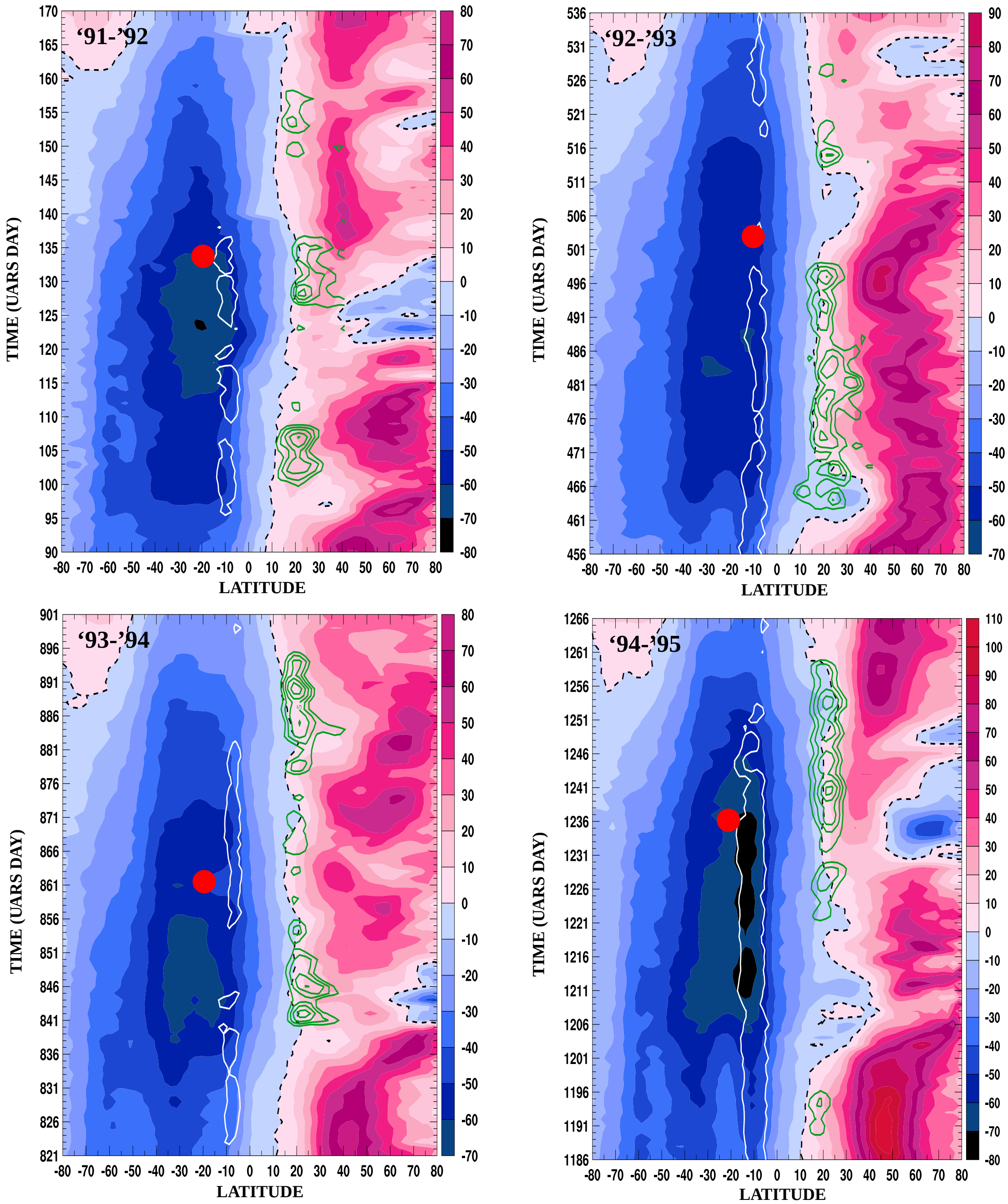

Figure 3. Time-evolution of the zonal-mean zonal winds at 1 mb from 10 December 1991 to 28 February 1992. The dashed line represents the zero-wind line. Superimposed are zero lines of zonal-mean quasi-geostrophic potential vorticity (PV) gradient (bold white line). The bold white line hence encloses the region of quasi-geostrophic PV gradient reversal. The peak of the 2-day wave temperature amplitude during the period studied (UARS days 123-155) is noted for reference (red dot). The green contours indicate the intensity of the inertial eddies, diagnosed as the meridional wind variance filtered for wave numbers 10-15 and periods longer than 7 days (see text). The three other panels are the corresponding graphs for 1992/1993, 1993/1994 and 1994/1995. In 1991/1992 and 1994/1995, the contours are from 6 to 10 by 1 m^2s^{-2}. In 1992/1993 and 1993/1994, the contours are 4 to 6 by 0.5 m^2s^{-2}.

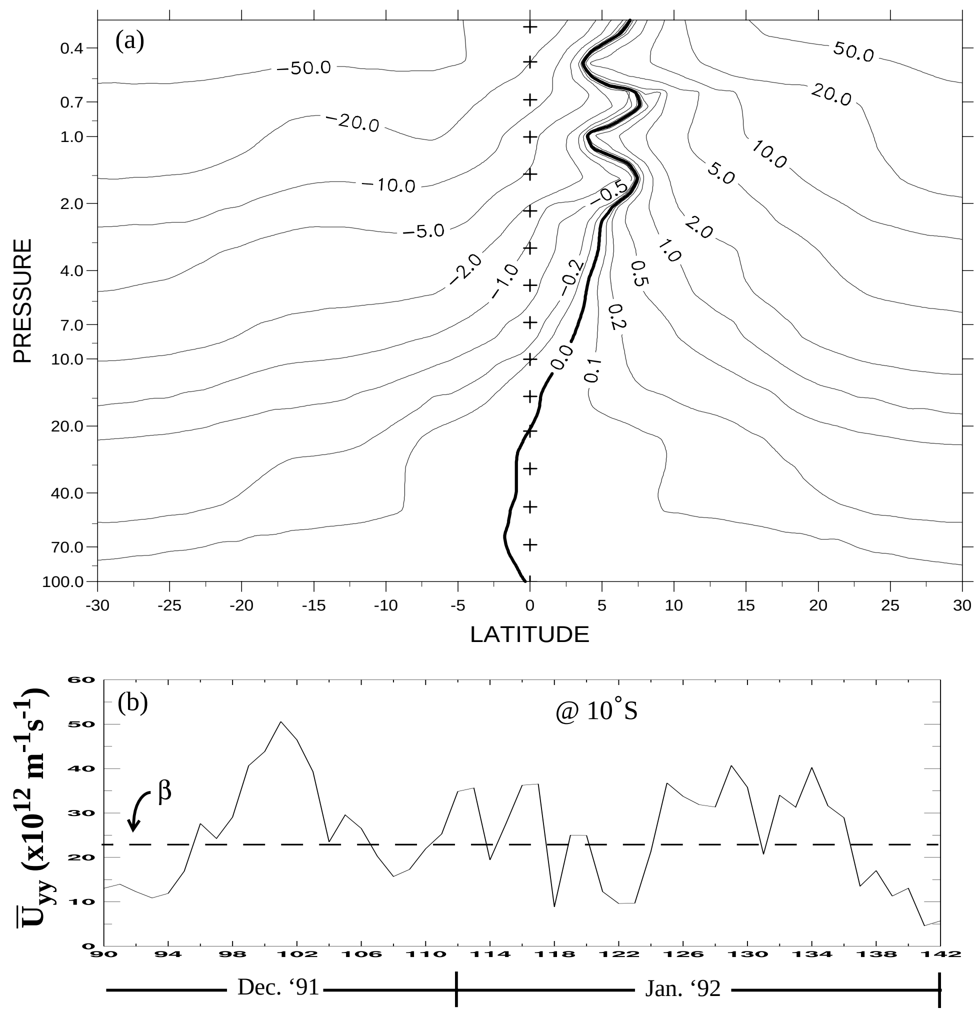

Figure 4. (a) Pressure/latitude cross-section of zonal-mean potential vorticity (PV) averaged over UARS days 126-132. The crosses indicate the standard UARS levels, where the analyses are archived. On this figure and hereafter, PV is in unit of 10^{-2} Km^2s^{-1} kg^{-1}. (b) Meridional curvature of the zonal-mean zonal wind as a function of time at 10˚S and 1 mb. The quantity β is indicated by the dashed bold line.

ance of 1 or 2 K^2, and occurring at 20˚S at the time indicated by the red dot on Fig. 3. The peak is seen to occur as the jet reaches its maximum strength, and after or coincident with a period of prolonged PV gradient reversal.

(e) Discussion

The pulsed character of the temperature wave, building in amplitude over approximately one week, its magnitude and its meridional confinement in the summer subtropics are in agreement with previous studies of National Meteorological Center analyses (Randel, 1994). The MLS temperature time series peaks about 6 days later than the one shown on Fig. 1(c) (see Fig. 2 of LL95).

Possible excitation of the 2-day wave by internal instability has been examined in analyses (Randel, 1994), in satellite observations (Burks and Leovy, 1986), and in numerical models of baroclinic instability (Plumb, 1983; Pfister, 1985) or barotropic instability (Manney *et al.*, 1988). General circulation models

(GCMs) of the middle atmosphere have also been shown to contain global westward propagating modes, including a 2-day wave (Hunt, 1981; Manzini and Hamilton, 1993; Norton and Thuburn, 1996). Interestingly, Manzini and Hamilton (1993) showed that the global westward modes in their GCM were not forced by tropospheric latent and convective heating. In the GCM study of Norton and Thuburn (1996), the 2-day wave originated in an instability of the mesospheric jet structure.

Above 1 mb, the 2-day wave perturbation decays in the analyses, while MLS and LIMS observations revealed a perturbation growing with height from above 2 mb up to the last analyzed level (Burks and Leovy, 1986; LL95). Above the stratopause, there are little temperature observations injected into the analyses, and, furthermore, momentum dissipation by the Rayleigh drag is likely to alter the wave structure.

4. Inertial circulations in the winter subtropics

(a) Isentropic transport of water vapour

The planetary scale waves in the tracer summer hemisphere distribution are to be contrasted with the more vigorous eddies on the less-than-planetary scales in the winter hemisphere. First, Figs. 2(a) and (b) show a wide dry tongue drawn out of the tropics into the NH in the longitude range 225˚E-275˚E (see thick arrow on Fig. 2(b)). It is caused by the mid-January sudden warming. In addition, thin streamers of water vapour are mixed in longitudinally-narrow (zonal wave number 10-12 approximately) gyres (Fig. 2(a),(b),and (c); thin arrows on Fig. 2(b)). Some water vapour filaments are actually drawn out of the SH into the gyres, and roll up near 20˚N (see left-most arrow on Fig. 2(b)).

Two additional simulations were carried out during period A at 1800 K and 2100 K, but using latitude as an initial tracer field. Figure 5(a) is a close-up on the gyre seen on 17 January near 150˚E (see Fig. 2(b)), but the latitude tracer indicates the meridional origin of fluid material drawn into the eddy. Figure 5(b) is analogous to Fig. 5(a) but at 2100 K, i.e. near 0.7 mb. The transport model resolution makes it possible to capture the detailed wrapping of isopleths in such eddies. On Fig. 5(b), the thick contours enclose tracer in the gyre, which did originate in the SH.

(b) Spectral analysis of meridional winds

In order to characterize the occurrence and strength of these eddies, we spectrally analyzed the meridional wind over a 80-day period starting UARS day 90, and over a latitude range of 5˚S to 45˚N. The resynthesized variance is shown on Fig. 3 (green contours on upper-left panel), after filtering for wave numbers 10 to 15, and periods longer than 5 days, corresponding to eddies seen on tracer transport maps. These high wave number eddies are seen to intensify sporadically throughout winter, just after periods of intense mid-latitude wave activity, such as the sudden warming of mid-January 1992. These eddies are centered near 20˚N. Note their appearance after periods of cross-equatorial shear enhancement.

(c) Signature on potential vorticity

In the UKMO analyses, the zonal-mean PV structure near the stratopause in the northern subtropics is quite remarkable. The region of negative PV penetrating into the NH covers all heights above 10 mb (Fig.4(a)). More interestingly, the zero-PV line has a wavy vertical structure above 2 mb. This undulating structure in the zero-PV contour is not so strong in the following week, as the extratropical wave activity diminishes.

These deformations of the PV contours however are zonally asymmetric: Figs. 6(a) and (b) show the PV longitude-latitude maps at 1 and 0.68 mb, averaged over UARS days 126-132. A running mean over 15˚ in longitude, and over 5˚ in latitude has been applied before plotting. There is a very large difference in

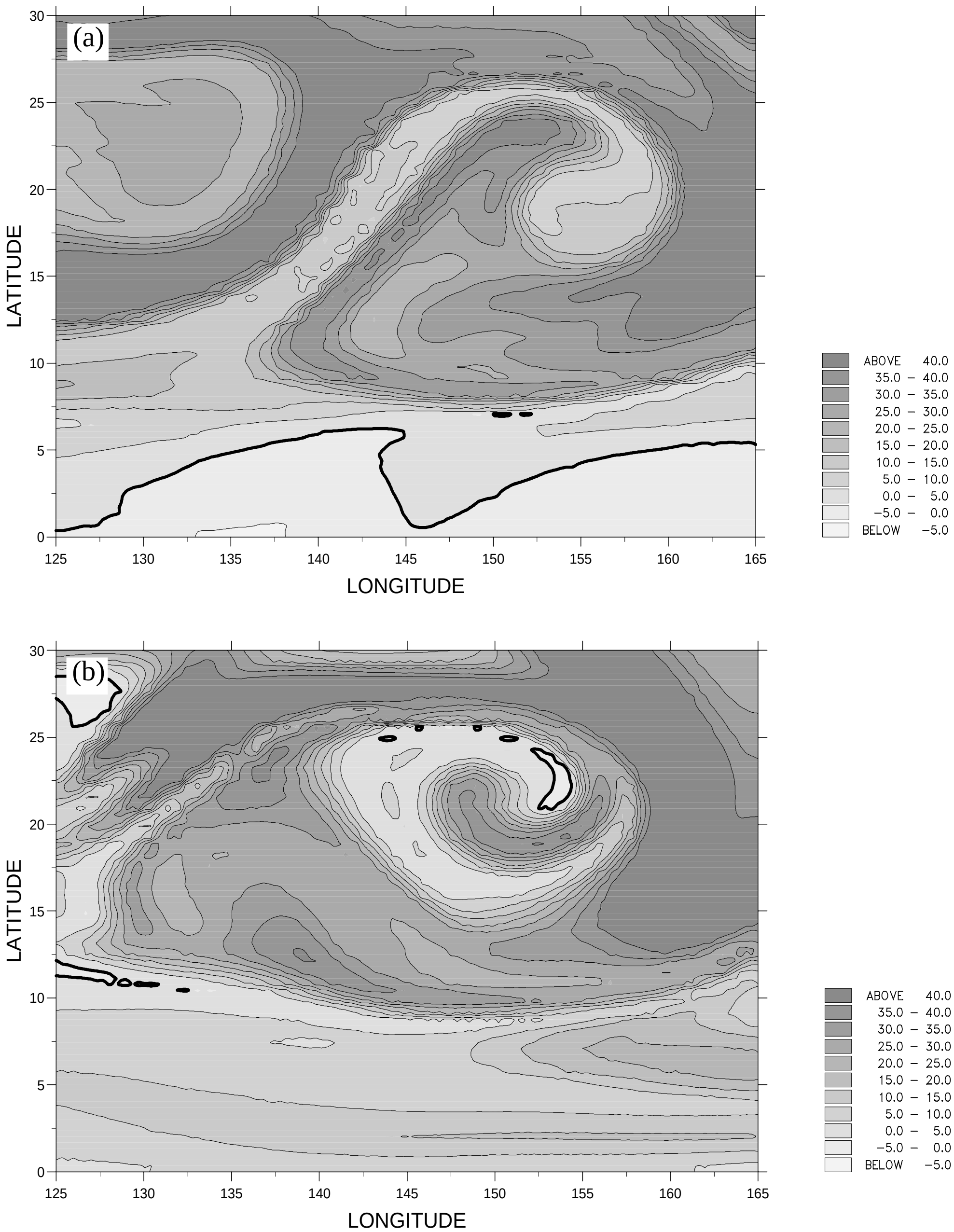

Figure 5. Distribution of the “latitude” tracer at 1800 K on (a) 17 January 1992, (12 GMT), closing up on the gyre seen near 150˚E on Fig. 2(b). (b) Same as (a) but at 2100 K. The bold line is the zero latitude contour. Contour spacing corresponds to 5˚.

the position of the zero-PV contour at these levels in the longitude range 100˚E-225˚E: it is strongly displaced equatorward at 1 mb, and poleward at 0.68 mb. Hence, PV is larger near the equator at 1 mb than at 0.68 mb in that longitude range. Note also the tongue of low PV in the northern subtropics near 250˚E-300˚E, which is advected northward in association with the wave breaking pattern during the sudden warming event.

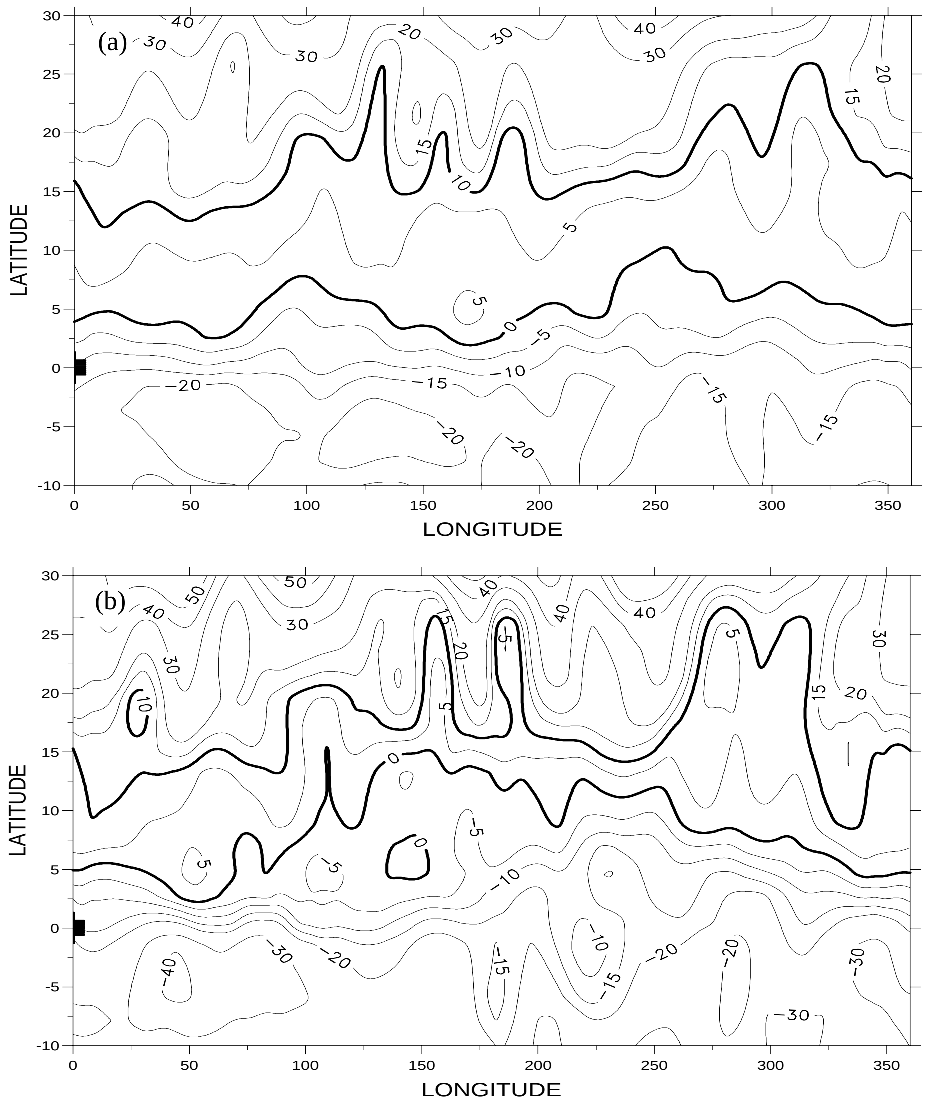

Figure 6. Latitude/longitude map of potential vorticity, averaged over UARS days 126-132, at (a) 1 mb and (b) 0.68 mb.

(d) Results for other UARS years

A similar analysis was carried for the 3 subsequent northern hemisphere winters (Fig. 3). High wave number eddies confined near 20˚N are seen to intensify sporadically after periods of intense mid-latitude eddy activity. However, the amplitude of these eddies is highly variable from one year to the other. Stronger eddies were observed in 91/92 and 94/95, two years characterized by major warmings.

(e) Discussion

The salient characteristics of these eddies are: (i) the timing of their occurrences after intense mid-latitude wave activity, the associated deformation of the zonal mean flow, and enhancement of cross-equatorial shear, (ii) the stacked vertically-narrow patterns in potential vorticity near the low latitude stratopause, (iii) their turnover time estimated to about 3 or 4 days, close to the inertial period of about 3 days at 10˚N, and 5 days at 5˚N, (iv) their less-than-planetary scale (zonal wave number 10 to 15).

These characteristics of these fully-developed eddies are reminiscent of inertial instabilities, although secondary high wave number Rossby waves, induced near the zero-wind line might contribute to the tracer transport too.

Linear inertial instability of a parallel basic flow to either zonally symmetric or asymmetric modes has been considered by Dunkerton (1981,1983). In the real atmosphere, it is likely that zonally asymmetric instabilities will be associated with the deformation of the low latitude mean flow by extratropical Rossby wave breaking. The linear theory of such disturbances to a zonally-asymmetric basic flow has been explored only recently (Dunkerton, 1993; Clark and Haynes, 1996). Their longitudinal extent (approximately 30˚) is also compatible with the linear stability analysis of a parallel flow (Dunkerton, 1983), who found most unstable modes characterized by zonal wave numbers up to 12, depending on the mode vertical wavelength. Numerical models of the middle atmosphere also display zonally-asymmetric inertial circulations at low latitudes organized by Rossby wave breaking (O'Sullivan and Hitchman, 1992; Sassi *et al.*, 1993).

Theoretical studies of inertial instability predict that unstable modes with the smallest vertical length scale are favoured, but eddy viscosity excludes the unstable modes of infinite vertical wave number. In numerical models, inertially unstable modes would tend to have a vertical wavelength of twice the model vertical grid spacing. The analyzed data do not allow investigation of the vertical structure of these eddies, although meridional velocity locally exhibits strong variations from one UARS level to the next (not shown). In regions of the atmosphere where observations are sparse, assimilated data are a blend of coarse observations and model-generated features. The short horizontal and vertical scales of these inertial eddies implies that they are model-generated features. This does not mean that they are necessarily irrelevant. They might resemble in some ways undersampled processes occurring in the real atmosphere. Hence, the transport simulations, initialized with a zonally-averaged tracer, have to be understood as indicating where tracer filamentation is occurring, but not as realistically locating a given filament. There are enough observations to constrain however, where the large-scale tongue of tracer is eroded out of the tropics in association with the sudden warming.

The temperature anomalies observed by Hitchman *et al.* (1987), or the residual circulation computed by Sassi *et al.* (1993), extended into the mesosphere, and the current data, being archived up to 0.32 mb, may only capture the bottom inertial cells.

5. WATER VAPOUR UARS MLS MEASUREMENTS NEAR THE STRATOPAUSE IN NH WINTER 1991/92

Observational evidence for strong mixing in the NH subtropics is deduced from the water vapour measurements by the MLS instrument aboard UARS from December 1991 to February 1992.

A set of 9228 along-track profiles taken in the period 15-22 January (UARS days 126-132) is used. The satellite was not sounding north of 30˚N during this period. Validation of version 3 MLS water vapour data is provided by Lahoz *et al.* (1996). The vertical resolution is about 5 km. The accuracy in the upper stratosphere is about 10%.

All mixing ratios at 1 mb, measured between UARS day 126 and 132, are shown as a function of latitude on Fig. 7(a) (grey dots). Note the larger spread of the values in the NH subtropics compared to the SH subtropics. Moreover, along-track measurements from two particular orbits on UARS day 128 also show sharp variations well above the noise level, indicating the presence of features a few degrees wide in the along-track direction, in the latitude range 10˚N-25˚N.

To investigate the zonal asymmetries, mixing ratios at 1 mb from 3 consecutive days (UARS days

128-130) were interpolated (Fig. 7(b)) on a 2 × 2 longitude-latitude grid using a Gaussian weighting function with characteristic lengths of 3° in longitude and 2° in latitude (Dunkerton and O'Sullivan, 1996). The two orbital tracks corresponding to the thick lines in Fig. 7(a) are also plotted (crosses).

Obviously, the map is asynoptic, but it shows interesting features. (i) The deformation of the 6.4 and 6.2 parts per million by volume isopleths (shaded area) reveals longitudinal asymmetries. One sees a tongue eroded out of the tropics, centered near 350°E. Note that this tongue is well captured by passive tracer distributions derived from the UKMO analyses (see Figs. 2(a) and (b)). (ii) In the 50°E-250°E longitude range, repeated folding of the same isopleths near 20°N indicates strong mixing. Parcels with low water vapour content have been transported northward to 20°N-25°N.

The water vapour measurements were further binned in 5° wide bins, and the spread around the mean was calculated for each bin and each day from UARS day 90 to UARS day 170. Figure 7(c) shows the time-evolution of this spread. Note that, in the summer subtropics, there is a maximum coincident with the 2-day wave occurrence (see LL95). Plumb *et al.* (1987) argued that the 2-day wave was the most effective latitudinal transport process in the summer mesosphere. In the NH subtropics, near 20°N-30°N, periods of enhanced variability in observed water vapour are in good correspondence with periods of mid-latitude eddy activity in the UKMO analyses. In particular, the occurrence of the sudden warming (UARS day 125) corresponds to the time when the spread is maximum in the NH subtropics. These periods when the water vapour variability is enhanced in the NH subtropics are lasting one to two weeks, and roughly correspond to periods of strenghtened inertial eddies in the UKMO analyses (Fig. 3 upper left panel).

The UARS water vapour observations are too coarse to fully resolve eddies at zonal wave numbers higher than 7. All that can be said is that these observations suggest that gyres might mix water vapour across the subtropical meridional gradient, in a process like that indicated by Figs. 2(a) and (b).

6. A POSSIBLE LINK BETWEEN WINTER HEMISPHERE PLANETARY WAVES, INERTIALLY UNSTABLE DISTURBANCES, AND THE 2-DAY WAVE

Hitchman (1985) speculated that momentum redistribution by inertially unstable disturbances would alter the curvature of the mean zonal flow near the equator, contributing to barotropic destabilization of the summer easterlies. This could contribute to the onset of the 2-day wave. Wu *et al*. (1996) show evidence that the 2-day waves (wave numbers 3 and 4) are possibly linked to winter hemispheric planetary waves, the possible leakage of which into the summer hemisphere may enhance unstable modes of the summer easterly jet.

Our analysis of the UKMO data suggests a coupling mechanism which does not rely on the penetration of a particular wave mode into the opposite hemisphere. Planetary wave amplification altering the zonal-mean wind structure in the winter middle latitudes, and not necessarily full-blown sudden warmings, governs the activation of inertial instabilities, as described in section 4. In the following, we explain how the latter create a region of strong wind curvature in the summer subtropics, and conditions favourable for the genesis of the 2-day wave.

Horizontal momentum transports by inertial waves tend to produce westerly momentum convergence near the equator, slowing down the easterlies, and divergence near 10°N-15°N, weakening the westerlies (Hitchman *et al*., 1987). Figure 8 shows that, after gaining in intensity prior to UARS day 122, the equatorial zonal easterly flow gradually weakens. The period of weakened easterlies is associated with the onset of strong inertially unstable disturbances and contributes to a rapid increase in zonal-mean zonal wind meridional curvature near 10°S, which exceeds β. The series of zonal-mean zonal wind profiles at 1 mb illustrate more clearly this enhancement of the wind curvature near 10°S (Fig. 9): the wind profile on UARS day 125 is remarkable in showing an S-shaped profile centered near 5°N, which may result from such a momentum redistribution by the inertial eddies. The formation of the S-shaped profile contributes to the development of the reversal of the quasi-geostrophic PV gradient near 10°S. Hence it can be argued that inertially unstable disturbances provide the effective linkage between winter hemisphere planetary

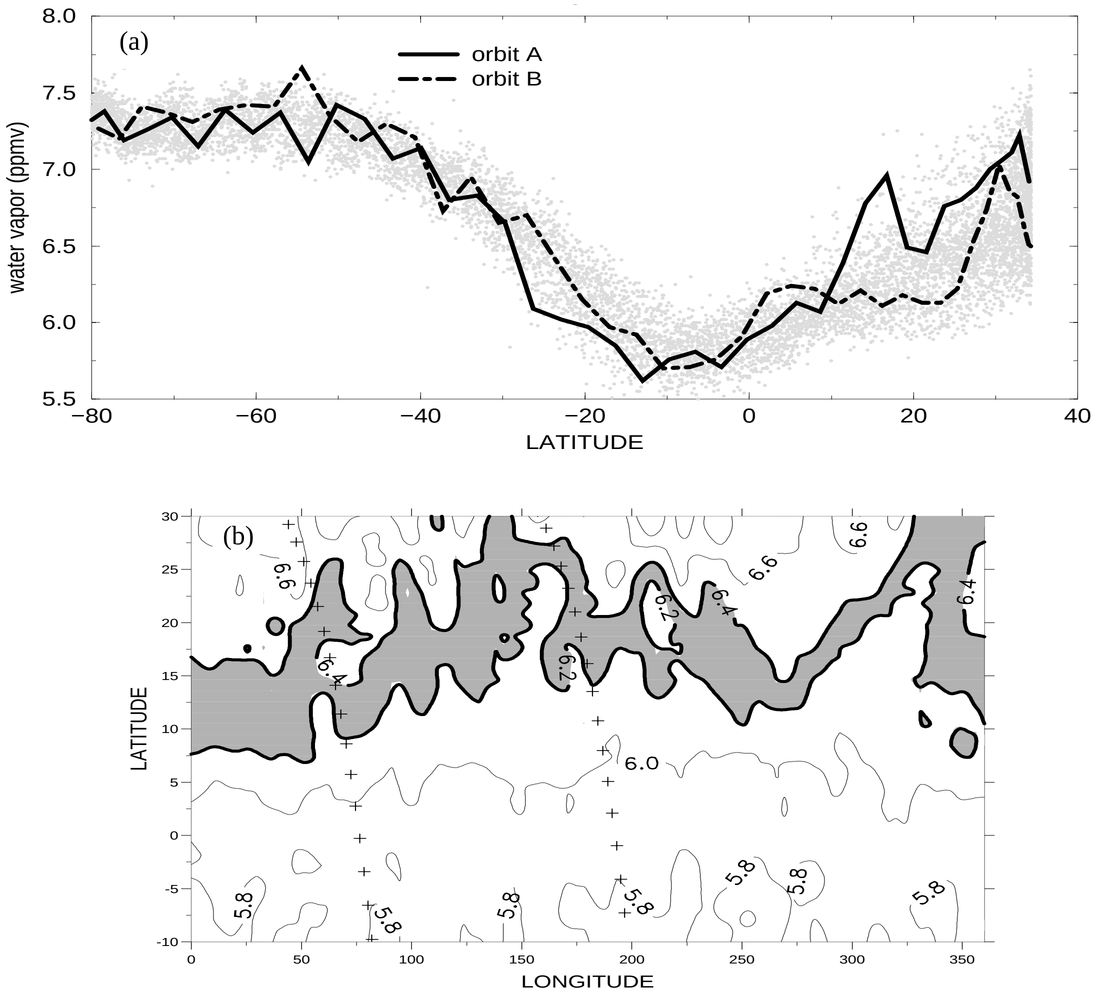

Figure 7. (a) Along-track water vapour MLS mixing ratio (p.p.m.v.) at 1 mb during UARS days 126-132, plotted as a function of latitude (gray dots). Measurements along two particular orbital tracks are also shown (thick lines). (b) Latitude/longitude map of the same quantity, using all the profiles retrieved during UARS days 128-130, at 1 mb. The crosses correspond to the thick lines in (a). (c) The day-to-day evolution of the spread (p.p.m.v.) around the mean in latitude bins (see text).

waves and 2-day waves. These profiles also show a decrease of the easterly jet maximum at 1 mb between UARS days 125 and 131, consistent with the onset of 2-day waves (Plumb *et al.*, 1987; Randel, 1994). Note however that in 1991/1992, reversal of the quasi-geostrophic PV gradient is observed on several occasions prior to UARS day 125, and it is likely that the suggested mechanism only provide conditions favourable, i.e. not sufficient, to the onset of 2-day wave.

7. Summary

The 2-day wave is a dominant wave-like feature of the upper atmosphere summer circulation, and there exists an abundant literature on its signature, in particular in the radar community. It has been sug-

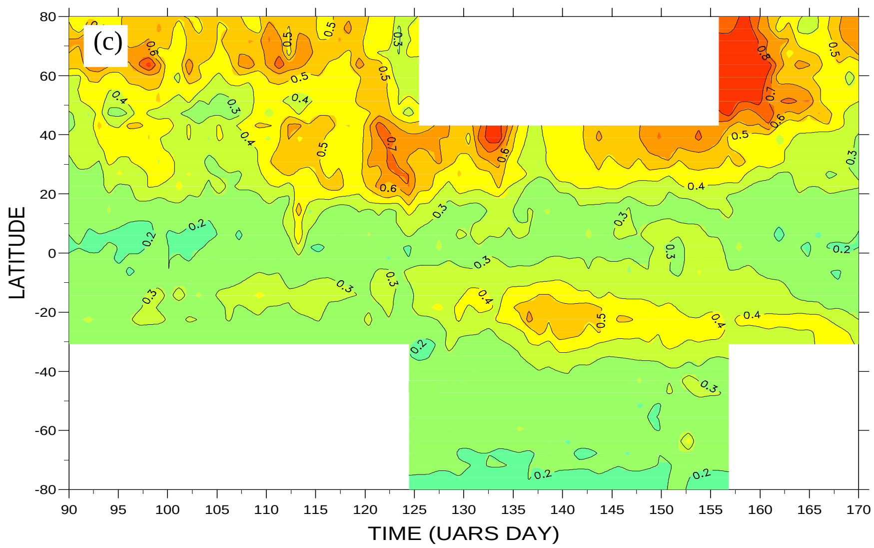

Figure 7. Continued.

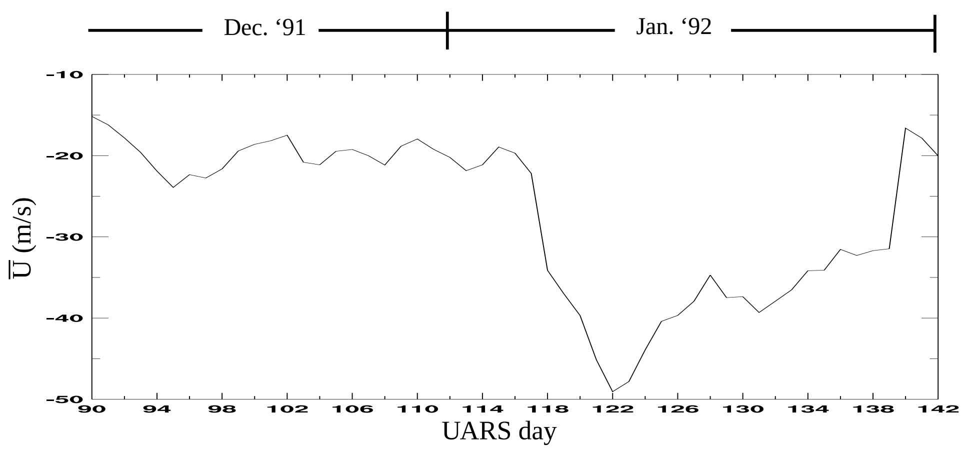

Figure 8. Evolution of the zonal-mean zonal wind at the equator and 1 mb for UARS days 90-142.

gested to originate in an internal instability of the westward summer jet, to be a global normal mode (see Hagan *et al*., 1993 and references therein), or to be a near-resonant mode excited by internal instability. Our spectral analysis of assimilated wind and temperature reveals that the summer tropical upper stratosphere contains large planetary waves, including a prominent 2-day wave, as well as a wave-1 of period near 7 days.

The occurrence of the 2-day wave in the present study seems to coincide with a zonal-mean PV gradient reversal near 1 mb. Generation near the stratopause is by no means contradictory with the existence of 2-day wave signals in the mesosphere and lower thermosphere, as the wave may propagate upwards through more westerly flow.

If the summer hemisphere low latitudes are dominated by planetary scale waves, albeit of large amplitude and breaking, there is, on the contrary, considerable mixing on the less-than-planetary scales in the winter subtropics. In the NH subtropics, eddies possibly linked to inertial instabilities appear clearly in the water vapour transport simulation, and this is confirmed by the strong zonal variability in the observed

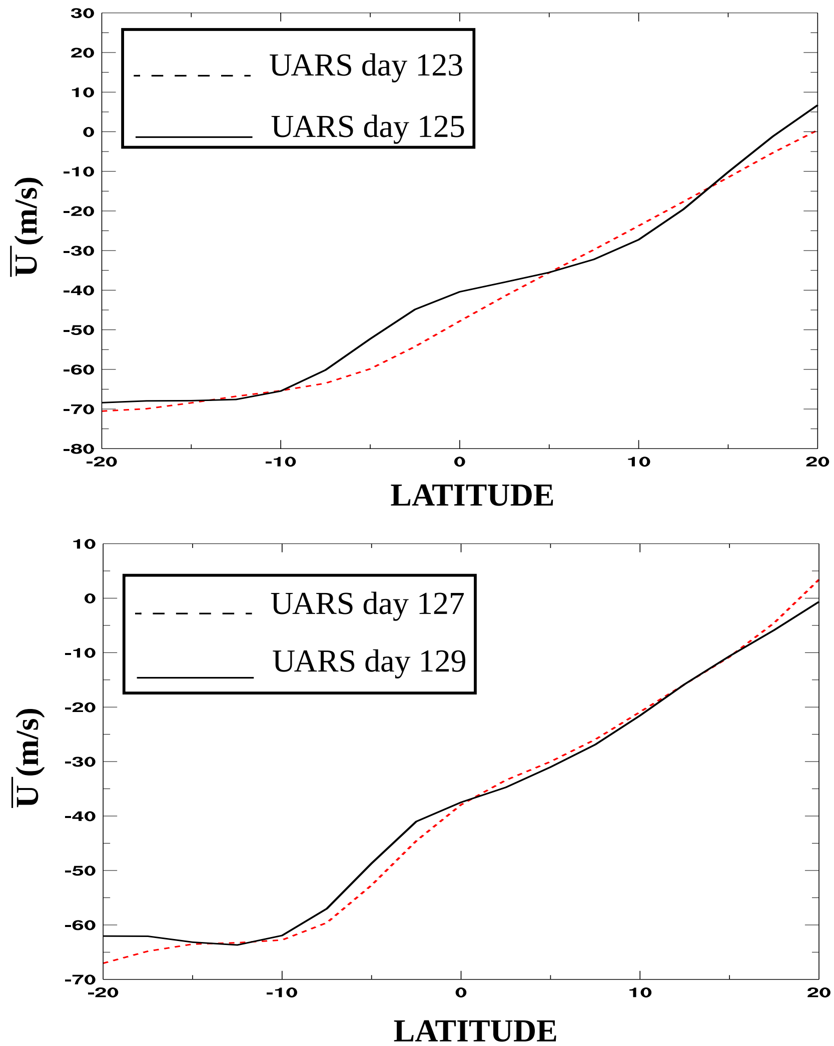

Figure 9. Meridional profiles of zonal-mean zonal wind at 1 mb for several individual days.

water vapour.

The current analysis suggests that planetary wave activity in the winter hemisphere leads to the generation of the 2-day wave in the opposite hemisphere, by enhancing inertial circulations in the tropics.

The UKMO analyses, used in this study, do not faithfully picture the mesospheric jets, hence may under-represent baroclinically unstable shear zones above the core of the summer jet. Nevertheless, it can be inferred that the climatologically stronger wave activity in the NH, would be the reason why the 2-day wave is stronger in January-February than in July-August. The unstable modes of the stronger SH summer jet would also be of shorter period, in qualitative agreement with observations of a longer 2-day wave during the NH summer.

ACKNOWLEDGEMENTS

This work was carried out while the first author was a Visiting Scientist at the CNRM. This work was partially supported by the French Middle Atmosphere Program, and by the NASA Upper Atmosphere Research Satellite Program under grant number NASS-26301. The authors acknowledge the UK Meteorological Office for making the data available. The data were retrieved from the British Atmospheric Data Centre and NASA Goddard DAAC database. One author (Y. O.) would also like to thank P. Simon and M. Amodei for lending their tracer transport and spectral analysis codes, and Richard Swinbank and Dr. John Stanford for useful comments.

REFERENCES

Burks D. and Leovy, C. B. 1986 Planetary Waves near the Mesospheric Easterly Jet, *Geophys. Res. Lett.*, **13**, 193-196.

Clark P. D. and Haynes, P. H. 1996 Inertial instability on an asymmetric low-latitude flow, *Quart. J. Roy. Met. Soc.*, **122**, 151-182.

Dunkerton, T. J. 1981 On the inertial stability of the equatorial middle atmosphere, *J. Atmos. Sci.*, **38**, 2354-2364.

1983 A nonsymmetric equatorial inertial instability, *J. Atmos. Sci.*, **40**, 807-813.

1993 Inertial instability of a nonparallel flow on an equatorial β plane, *J. Atmos. Sci.*, **50**, 2744-2758.

Dunkerton, T. J. and O'Sullivan, D. J. 1996 Mixing zone in the tropical stratosphere above 10 mb, *Geophys. Res. Lett.*, **23**, 2497-2500.

Farman J. C., O'Neill, A., and Swinbank, R 1994 The dynamics of the arctic polar vortex during the EASOE campaign, *Geophys. Res. Lett.*, **21**, 1195-1198.

Hagan, M. E., Forbes, J. M., and Vial F. 1993 Numerical investigation of the propagation of the quasi-2-day wave into the lower thermosphere, *J. Geophys. Res.*, **98**, 23193-23205.

Hitchman, M. H. 1985 'An observational study of wave-mean flow interaction in the equatorial middle atmosphere', *Ph.D. Thesis*, University of Washington.

Hitchman, M. H.and Leovy, C. B. 1986 Evolution of the zonal mean state in the equatorial middle atmosphere during October 1978-May 1979, *J. Atmos. Sci.*, **43**, 2219-2236.

Hitchman, M. H., Leovy, C. B., Gille, J. C., and Bailey, P. L. 1987 Quasi-Stationary Zonally Asymmetric Circulations in the Equatorial Lower Mesosphere, *J. Atmos. Sci.*, **44**, 2219-2236.

Hunt, B. G. 1981 The maintenance of the zonal mean state of the upper atmosphere as represented in a three-dimensional general circulation model extending to 100 km, *J. Atmos. Sci.*, **38**, 2172-2186.

Lahoz, W. A., Suttie, M. R., Froidevaux, L., Harwood, R. S., Lau, C. L., Lungu, T. A., Peckham, G. E., Pumphrey, H. C., Read, W. G., Shippony, Z., Suttie, R. A., Waters, J. W., Nedoluha, G. E., Oltmans, S. J., Russell III, J. M., and Traub, W. A. 1996 Validation of UARS MLS 183 Ghz H_20 measurements, *J. Geophys. Res.*, **101**, 10129-10149.

Limpasuvan, V. and Leovy, C. B. 1995 Observations of the Two-Day Wave near the southern summer stratopause, *Geophys. Res. Lett.*, **22**, 2385-2388.

Manney, G. L., Nathan, T. R., and Stanford, J. L. 1988 Barotropic stability of realistic stratospheric jets, *J. Atmos. Sci.*, **45**, 2545-2555.

Manzini E. and Hamilton K. 1993 Middle Atmospheric Traveling Waves Forced by Latent and Convective Heating, *J. Atmos. Sci.*, **50**, 2180-2200.

Norton, W. A., and Thuburn J. 1996 The 2-day wave in a middle atmosphere GCM, *Geophys. Res. Lett.*, **23**, 2113-2116.

O'Sullivan, D. J, and Hitchman, M. H. 1992 Inertial instability and Rossby wave breaking in a numerical model, *J. Atmos. Sci.*, **49**, 991-1002.

Orsolini, Y. J. 1995 On the formation of ozone laminae at the edge of the Arctic polar vortex, *Quart. J. Roy. Met. Soc.*, **121**, 1923-1941.

Pfister, L. 1985 Baroclinic instability of easterly jets with applications to the summer mesosphere, *J. Atmos. Sci.*, **42**, 313-330.

Plumb, R. A. 1983 Baroclinic Instability of the Summer Mesosphere: A Mechanism for the Quasi-Two-Day Wave?, *J. Atmos. Sci.*, **40,** 262-270.

Plumb, R. A., Vincent, R. A., and Craig, R. L. 1987 The quasi-two day wave event of January 1984 and its impact on the mean mesospheric circulation, *J. Atmos. Sci.*, **44**, 3030-3036.

Randel, W. J. 1994 Observations of the 2-Day Wave in NMC Stratospheric Analyses, *J. Atmos. Sci.*, **51**, 306-313.

Sassi F., Garcia, R. R., and Boville, B. A. 1993 The stratopause semiannual oscillation in the NCAR Community Climate model, *J. Atmos. Sci.*, 50, 3608-3624, 1993.

Swinbank, R. and O'Neill, A. 1994a A Stratosphere-Troposphere Data Assimilation System, *Mon. Wea. Rev.*, **122**, 686-702.

1994b Quasi-biennial and semi-annual oscillations in equatorial wind fields constructed by data assimilation, *Geophys. Res. Lett.*, **21**, 2099-2102.

Wu D. L., Hays, P. B., Skinner, W. R., Marshall, A. R., Burrage, M. D., Lieberman, R. S., and Ortland, D. A. 1993 Observations of the quasi-2-day wave from the high resolution Doppler imager on UARS, *Geophys. Res. Lett.*, **20**, 2853-2856.

Wu, D. L., Fishbein, E. F, Read, W. G., and Waters, J. W. 1996 Excitation and Evolution of the Quasi-2-Day Wave Observed in UARS/MLS Temperature Measurements, *J. Atmos. Sci.*, **53**, 728-738.